Journal of the Korean Physical Society, Vol. 76, No. 4, February 2020, pp. 297∼300

# Emission Characteristics of Charged Particle Production in Interactions of $^{84}$Kr with the Nuclear Emulsion Detector at Relativistic Energy

U. Singh and M. K. Singh*
*Department of Physics, Institute of Sciences and Humanities, G. L. A. University, Mathura 281406, India*

V. Singh
*Department of Physics, Institute of Science, Banaras Hindu University, Varanasi 221005, India and*
*Department of Physics, School of Physical and Chemical Sciences,*
*Central University of South Bihar, Gaya 824236, India*

(Received 9 August 2019; revised 31 October 2019; accepted 4 November 2019)

This article focuses on the characteristics of the charged particle produced in nucleus-nucleus collisions at relativistic energy. We have studied the emission behavior of charged particles observed in the forward hemisphere ($\theta < 90^\circ$) and the backward hemisphere ($\theta \geq 90^\circ$). This study shows that the charged particles produced in the forward hemisphere strongly depend on the mass of the projectile beam whereas in the backward hemisphere, they show an exponential decay behavior and are independent of the mass of the projectile beam. The results are compared with other experimental observations and found to be consistent.

PACS numbers: 25.70.Mn, 29.40.Rg, 25.70.Pq
Keywords: $^{84}Kr_{36}$-emulsion interactions, Nuclear emulsion detector, Emission characteristics of shower particles
DOI: 10.3938/jkps.76.297

## I. INTRODUCTION AND PHYSICS MOTIVATION

The nuclear emulsion detector has played an important role in high energy interaction physics, and it has been in use since the birth of experimental nuclear physics [1, 2]. The compactness of size, $4\pi$ detection capability, and better position resolution (less than 1 μm) make it a unique detector in nuclear experimental physics [1–3]. The study of heavy-ion collisions provides a unique opportunity to understand physics behind the state of matter under extreme conditions of density and temperature [1–3].

According to the Participant Spectator Model (PS Model) [4–7], the interacting system in relativistic nucleus-nucleus collisions can be divided into three main regions: First is the participants region which is the region of the two colliding nuclei. The velocity of this region has a wide distribution going from zero to the velocity of the projectile. Mostly, violent collisions happen in the participant region. Due to the strong interaction between the nucleons of the projectile and target in the participant region the fragments of this region are emitted at all center-of-mass angles into entire momentum range allowed by the kinematics in the center-of-mass frame [7]. In this region the energy transfer between two colliding nuclei is much higher than the nuclear binding energy. The second region is the projectile spectators region: In this region, the velocities of the emitted particles are almost the same as that of the projectile beam. Third is the target spectators region: In this region, the velocities of the emitted particles in the laboratory reference frame are almost zero [7–9]. The momentum transfer in both spectator regions (projectile and target) is very small compared to that the participant region. The PS Model predicts a clear-cut separation of the participants and the spectators regions because of the assumption of a clean geometry, which suggests that the nucleons in an overlapping volume participate in the reaction while spectators remain unaffected. A schematic diagram of the PS Model is shown in Fig. 1.

The spectators and participants regions of two colliding nuclei are correlated to each other. The liquid-gas phase transition is expected to happen in the spectator regions, and a quark gluon plasma (QGP) will be formed in the participants region at very high incident energies [10–12]. If the nuclear reaction mechanism is to be studied, the fragmentation mechanism of the participants region must be investgated. Therefore the study of the particles emitted from the participants region will reveal important information about the nuclear reaction

*E-mail: singhmanoj59@gmail.com

 

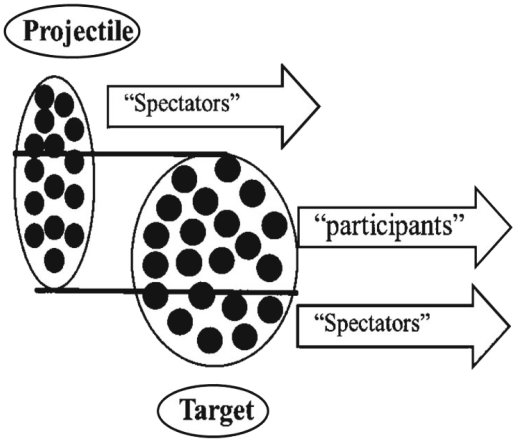


Fig. 1. Schematic diagram of PS Model.

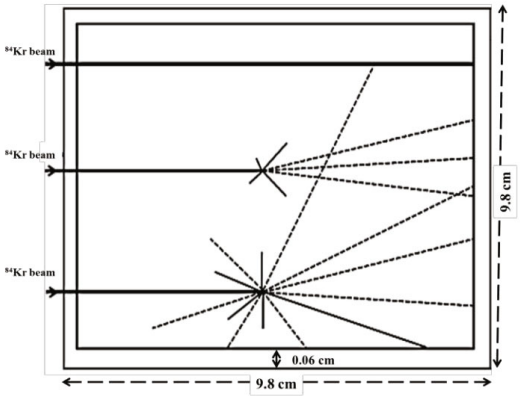


Fig. 2. Sketch of the stack showing the incident beam and the fiducial volume for scanning.

mechanism [7].

The present work focuses on the emission characteristics of the charged particles produced in the participants region of the collision. We have studied the emission behavior of shower particles in the forward hemisphere region ($\theta < 90^\circ$) and the backward hemisphere region ($\theta \geq 90^\circ$) produced in by interaction of $^{84}$Kr with an nuclear emulsion at $\sim$ 1 A GeV, and our results are consistent with other experimental observations [13,14].

## II. EXPERIMENTAL DETAILS

The exposure of the nuclear emulsion detector was performed at Gesellschaft fur Schwerionenforschung (GSI) Darmstadt, Germany. The $^{84}$Kr nuclei used as projectiles had a kinetic energy of $\sim$1 GeV per nucleon, with approximately 95 to 98% of $^{84}$Kr with no more than 5 to 2% of impurities. The target used was a highly sensitive NIKFI BR-2 nuclear emulsion detector. The nuclear emulsion detector was made of microcrystals of silver halides, especially Ag, Br, C, N, O and H, with small percentages of S and I dispersed in a very thin ($\sim$ 600 μm) layer of gelatine. The sizes of the microcrystals varied from 0.2 to 0.3 μm, the concentration of the crystals in the emulsion varied from 25% to 50% in volume, and the thickness of the emulsion layer was varied from 25 to 500 μm, depending on the specific use [7–9,15].

When ionizing particles traverse a nuclear emulsion layer, they creates electron-hole pairs in the crystals. Clusters of several silver atoms are formed in several microcrystals by successive ionic processes. The small silver clusters (known as latent images), are almost stable in time. Later they are amplified by the developer, so silver clusters with diameters of around 0.6 μm are formed. After the developing process (which was followed by fixing, washing and drying to remove the undeveloped crystals), the latent images changed into silver specks. A sketch of a stack showing the incident beam and the fiducial volume for scanning is shown in Fig. 2. The high-magnification Olympus BH-2 transmitted light-binocular microscope shown in Fig. 3 was used to magnify and measure the tracks of different particles in the nuclear emulsion detector at home institute [3].

Two standard methods was used for scanning events of interest [3]. The first is the line scanning method. In this method, the events of interest are scaned along the incident beam until they interact with or escape from the emulsion plate [3]. the second is the volume scanning method. In this method, events are scanned strip by strip. The volume scanning method is useful in the low-energy region where the number of events is much less [3]. The number of events used for this analysis was 700. All secondary charge particles are classified according to their range, velocity and ionization into following categories [3, 7–9, 15]: Shower particles are the freshly created (newly produced) charged particles, and have a normalized grain density less than 1.4 and a relative velocity more than 0.7. These particles are mostly pions with a very small mixture of kaons. The number of these particles is represented by the symbol $N_s$ [3,7–9]. Grey particles mainly come from the target spectator region and have a range in the emulsion plate of more than 3 mm, a normalized grain density between 1.4 and 6.0, and a relative velocity from 0.3 to 0.7 [3,7–9]. The number of these particles is denoted by the symbol $N_g$. Black particle have a range in the emulsion plate of less than 3 mm, a normalized grain density of more than 6.0 and a relative velocity less than 0.3. These are evaporated nucleons from the target [3,7–9]. The number of these particles is denoted by the symbol $N_b$. Heavily-ionized charged particles are grey particles and black particles together [3,7–9].

The projectile fragments mostly come from the projectile spectator region and have charges Z $\geq$ 1. These projectile fragments are further classified into three main divisions [3,7,9]: (i) single-charge projectile fragments ($N_{z=1}$) [8], (ii) double-charge projectile fragments ($N_{z=2}$) [8], and (iii) multiple-charge projectile fragments

Fig. 3. Photo of the Olympus BH-2 transmitted light-binocular microscope [3].

$(N_{z\geq 3})$ [8].

## III. RESULTS AND DISCUSSION

In the present study, we identify the shower particles produced in the interaction of $^{84}$Kr with a nuclear emulsion at 1 GeV per nucleon by using the techniques described above. Figure 4 shows the variation of the average number of shower particles with respect to the mass of projectile beam for different projectiles having masses in the between 7 and 132. From Fig. 4, we can see that the numbers of emitted shower particles linearly increase with increasing mass of the projectile beam. The increase in the emission of shower particles is proportional to the size of the participant region [3], and the size of participant region is proportional to the projectile size (mass) [7]. Thus, clear from Fig. 4, as the projectile size is increasing the participant region will increase, and the increase in participants will increase the number of freshly created (newly produced) particles. Figure 4 also shows that the emission of shower particles is independent of the incident kinetic energy of the projectile beam. These results are consistent with the other experimental observations [13,14].

We have studied the emission behavior of shower particles produced in the forward hemisphere ($\theta < 90°$) and the backward hemisphere ($\theta \geq 90°$). Figure 5 shows the emission probability of the shower particles in the backward hemisphere produced in the interaction of the nuclear emulsion (*i.e.*, same target) with various projectiles having masses between 7 to 84. From Fig. 5, we observe that the probability of emission of shower particles in the backward hemisphere is exponentially decreasing for all projectiles. Thus, the emission probabilities of shower

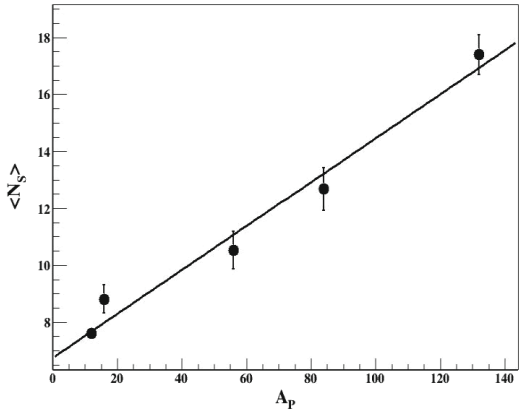


Fig. 4. Variation of the average number of shower particles with respect to the mass of the projectile beam for $^{12}$C (3.7 A GeV) [16], $^{16}$O (3.7 A GeV) [18], $^{56}$Fe (1.8 A GeV) [17], $^{84}$Kr (1 A GeV) [Present work], $^{132}$Xe (1.0 A GeV) [17].

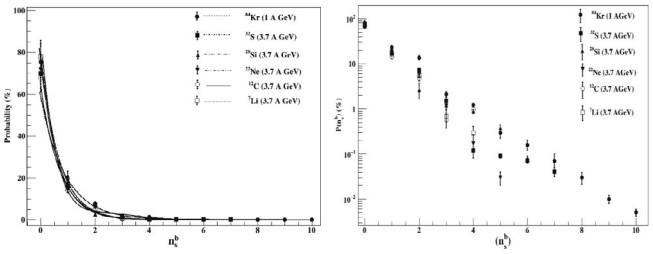


Fig. 5. (a) Probability distribution of shower particles produced in the backward hemisphere in the interaction of nuclear emulsion (*i.e.*, same target) with projectile beams of $^{7}$Li (3.7 A GeV), $^{12}$C (3.7 A GeV), $^{22}$Ne (3.7 A GeV), $^{28}$Si (3.7 A GeV), $^{32}$S (A GeV) [13], and $^{84}$Kr (1 A GeV) [Present work]. (b) Same figure on a different scale to make the data clearer.

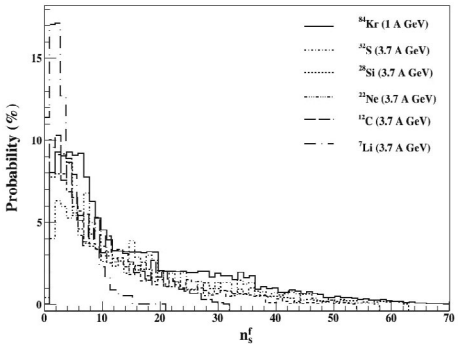


Fig. 6. Probability distribution of shower particles produced in the forward hemisphere in the interaction of nuclear emulsion (i.e. same target) with projectile beams of $^{7}$Li (3.7 A GeV), $^{12}$C (3.7 A GeV), $^{22}$Ne (3.7 A GeV), $^{28}$Si (3.7 A GeV), $^{32}$S (3.7 A GeV) [13], and $^{84}$Kr (1 A GeV) [Present work].

particles in the backward hemisphere are almost independent of the mass and the incident kinetic energy of the projectile beam [13,14].

Figure 6 shows the probability distribution of shower

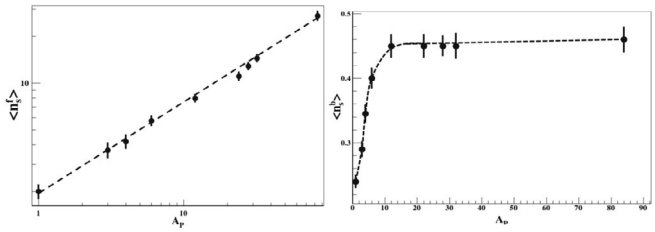

Fig. 7. Variation of the average multiplicity values of the (a) forward and the (b) backward emitted shower particles as functions of the mass of the projectile beam ($A_P$) for p (3.7 A GeV), $^{3}$He (3.7 A GeV), $^{4}$He (3.7 A GeV), $^{6}$Li (3.7 A GeV), $^{12}$C (3.7 A GeV), $^{22}$Ne (3.3 A GeV), $^{28}$Si (3.7 A GeV), $^{32}$S (3.7 A GeV) [13], and $^{84}$Kr (1 A GeV) [Present work].

particles produced in the forward hemisphere in the interaction of nuclear emulsion with different projectile beams having different incident kinetic energies. From Fig. 6, we observe that the distribution becomes broader with increasing projectile mass and incident kinetic energy [13,14]. This emission characteristic of shower particles reveals that they are mostly produced as a result of energy transfer to participating nucleons from the projectile [13]. This study shows that the emission probability of freshly produced particles in the interaction of two colliding nuclei is maximum in the forward hemisphere and minimum in the backward hemisphere.

Figure 7(a) shows the variation of the average multiplicity for $< n_s^f >$ as a function of the mass of a projectile beam of p, $^{3}$He, $^{4}$He, $^{6}$Li, $^{12}$C, $^{22}$Ne, $^{28}$Si, $^{32}$S and $^{84}$Kr. Figure 7(a) reveals that the emission of shower particles strongly depends on the mass of the projectile beam. Figure 7(b) shows the variation of average multiplicity for $< n_s^b >$ as a function of the mass of a projectile beam of the same projectiles as for Fig. 7(a). From Fig. 7(b), we observe that the emission or production of shower particles in the backward hemisphere initially increases with increasing mass of the projectile beam and then reaches a value $\sim 0.4$ for $A_P \geq 6$, after which it becomes independent of the projectile mass and incident kinetic energy, showing a almost constant value for values of $A_P$ from 12 to 84. This also proves physics behind Fig. 5 and Fig. 6.

## IV. CONCLUSION

In the present article, we have reported our study on the emission characteristics of the shower particles produced in the interaction of $^{84}$Kr with a nuclear emulsion at 1 GeV per nucleon. The study shows that the emission of shower particles linearly increases with increasing mass of the projectile beams, as shown in Fig. 4. Because the increase in the mass of the projectile beam will increases the participant region, the energy transfer of participating nucleons from the projectile beam will increases as the emission of shower particles increases.

## ACKNOWLEDGMENTS

The authors are grateful to the technical staff of GSI, Germany, for exposing the nuclear emulsion detector to a $^{84}Kr_{36}$ beam.

## REFERENCES

[1] W. H. Barkas, *Nuclear Research Emulsion* (Academic Press, London, 1963).
[2] M. K. Singh, Ramji Pathak and V. Singh, J. Purv. Acad. Sci. (Phys. Sci.) **15**, 166 (2009).
[3] M. K. Singh, Ph.D. thesis, VBS Purvanchal University, Jaunpur, India, 2014.
[4] M. Gauylassy and S. K. Kauffmann, Phys. Rev. Lett. **40**, 298 (1978).
[5] F. H. Liu, Chin. J. Phys. **38**, 1063 (2000).
[6] J. Knoll, J. Hufner and A. Bouyssy, Nucl. Phys. A **308**, 500 (1978).
[7] M. K. Singh, A. K. Soma, R. Pathak and V. Singh, Indian J. Phys. **85**, 1523 (2011).
[8] M. K. Singh, A. K. Soma, R. Pathak and V. Singh, Indian J. Phys. **87**, 59 (2013).
[9] M. K. Singh, A. K. Soma, R. Pathak and V. Singh, Indian J. Phys. **88**, 323 (2014).
[10] S. Ahmad *et al.*, Nature **403**, 581 (2000).
[11] J. Boguta, Phys. Lett. B **109**, 251 (1982).
[12] H. Weber, E. L. Bratkovskaya and H. Stocker, Phys. Lett. B **545**, 285 (2002).
[13] A. Abdelsalam, M. S. EI-Nagdy and B. M. Badawy, Can. J. Phys. **89**, 261 (2011), and references therein.
[14] W. Oswan *et al.*, J. Adv. Phys. **14**, 5213 (2018), and references therein.
[15] M. K. Singh, V. Singh and N. Bhatnagar, J. Korean Phys. Soc. **75**, 764 (2019).
[16] M. I. Adamovich *et al.*, Sov. J. Nucl. Phys. **29**, 52 (1979).
[17] N. Marimuthu *et al.*, Int. J. Mod. Phys. E **28**, 1950058 (2019).
[18] V. A. Antonchik *et al.*, Sov. J. Nucl. Phys. **40**, 483 (1984).